

Optical Interferometers with Reduced Sensitivity to Thermal Noise

H. J. Kimble,* Benjamin L. Lev,† and Jun Ye

JILA, National Institute of Standards and Technology and University of Colorado, Boulder, Colorado 80309-0440, USA
(Received 20 June 2008; published 30 December 2008)

A fundamental limit to the sensitivity of optical interferometry is thermal noise that drives fluctuations in the positions of the surfaces of the interferometer's mirrors, and thereby in the phase of the intracavity field. Schemes for reducing this thermally driven phase noise are presented that rely upon the coherent character of the underlying displacements and strains. Although the position of the physical surface fluctuates, the optical phase upon reflection can have reduced sensitivity to this motion. While practical implementation of such schemes for coherent compensation face certain challenges, we hope to stimulate further work on this important thermal noise problem.

DOI: 10.1103/PhysRevLett.101.260602

PACS numbers: 07.60.Ly, 04.80.Nn, 05.40.Ca, 42.62.Eh

Thermal noise presents a fundamental limit to measurement sensitivity in diverse areas of science and technology [1]. One important setting is that of optical interferometry in which otherwise stable structures experience small, thermally driven fluctuations in their dimensions in applications ranging from frequency metrology [2,3], to gravitational wave detection [4,5], to the realization of quantum behavior for macroscopic objects [6].

In some cases, the dominant limitation to length stability originates from thermally driven displacement noise for the reflective surfaces of the mirror substrates, and not from the supporting structure [2,3,5]. These fundamental fluctuations arise from substrate dissipation as demanded by the fluctuation-dissipation theorem (FDT) [7–9].

Beyond displacements driven by thermal noise in the substrate itself [10–15], diverse other sources of mechanical noise have been identified, including frictional losses in the materials that form the mirror coating [13,16], thermoelastic damping in the substrate and coating [15,17,18], and thermorefractive noise [19]. Measurements in rigid [2,3] and suspended interferometers [20–22] have confirmed many characteristics of such noise sources.

Various avenues have been followed for reducing thermal noise in optical interferometers, the most significant being lowering mechanical losses for the substrate [1,23] and, more recently, the coating [22,24]. New designs for advanced interferometers include the use of “coating-free mirrors” [25,26] and short Fabry-Perot (FP) cavities [27].

In this Letter, we propose a new strategy for reducing thermally driven phase noise in optical interferometers. Fundamental to our proposal is the observation that various manifestations of thermal noise can be coherent one with another. Our examples recognize that stochastic displacements δu_z perpendicular to the mirror's surface are necessarily accompanied by correlated strains and index changes in the materials of the mirror coating and substrate. Normally, the phase shift $\delta\beta$ due to these strains are small compared to the shift $\delta\theta$ from the surface motion δu_z . However, by suitable design, it is possible to achieve a total

phase shift $\delta\Phi = \delta\theta + \delta\beta \ll \delta\theta$ for the reflected field. That is, although the physical surface of the mirror is subject to random displacements δu_z , $\delta\Phi$ can have reduced sensitivity to these displacements with $\delta\theta$ coherently compensated by $\delta\beta$ from the coating and substrate. Although our current analysis is for “Brownian noise” of the substrate, our methodology should also be applicable to thermoelastic and coating noise as well.

As a first example, consider thermal noise for an eigenmode of a cylindrical mirror with mechanical resonance frequency ω_0 . For frequencies $\omega \simeq \omega_0$ and quality factor $Q_0 \gg 1$, microscopic thermal noise excites the entire “shape” of the relevant eigenmode $\xi_0(\mathbf{r})$, with a single, overall amplitude set by equipartition of energy [10,11]. The amplitude δu_z and accompanying strain ϵ_{zz} for thermally driven motion perpendicular to the mirror surface at $z = 0$ are then determined directly from $\xi_0(\mathbf{r})$.

Figure 1(a) illustrates a particular axisymmetric eigenmode $\xi_0(\mathbf{r})$ for a substrate of mass M as determined from a numerical finite-element analysis [28]. The end faces at $z = 0, l$ oscillate in opposition about the plane at $z = l/2$ with frequency ω_0 . At temperature T , δu_z at the central points $x, y = 0$ on the end faces have amplitude $\langle \delta u_z^2 \rangle_{\omega_0} \simeq k_B T / M_0 \omega_0^2$, where $M_0 = 2.7M$ is the effective mass for $\xi_0(\mathbf{r})$ [11]. Significantly, the axial strain per unit displacement $\zeta \equiv \epsilon_{zz}/u_z \simeq -1600/\text{m}$ at $\mathbf{r} = 0$ in Fig. 1(a).

Light reflected from the fluctuating surface of the substrate will be phase shifted. Following Levin [13], we introduce the displacement $q(z) = \int dx dy \delta u_z(r, z) \psi(r)$ weighted by the normalized intensity $\psi(r)$ over a plane at depth $z \geq 0$, where $\psi(r) = (2/\pi w_0^2) \exp(-2r^2/w_0^2)$ with $r = \sqrt{x^2 + y^2}$. The incident field with vacuum wave vector k experiences a phase change $\delta\theta = -2kq(z = 0) \equiv -2kq_0$ for the reflected field due to the surface's “piston” motion.

In addition to $\delta\theta$, strain that accompanies surface motion modifies the optical coating and thereby leads to a phase shift $\delta\beta$, with $\delta\beta$ expressed relative to the front surface of the coating. The overall phase shift for the

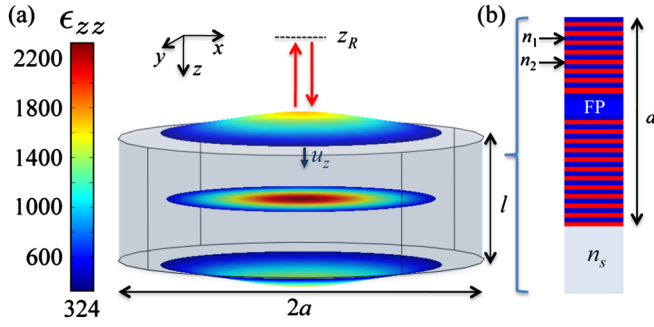


FIG. 1 (color online). (a) The undistorted shape of a substrate of radius $a = 1.5$ mm and thickness $l = 1$ mm is depicted by the shaded region and wire frame [28]. Axial displacements $u_z(x, y, z)$ and strains $\epsilon_{zz}(x, y, z)$ are shown across planes at $z = 0, l/2, l$ (top to bottom) for the eigenmode $\xi_0(\mathbf{r})$ with eigenfrequency $\omega_0/2\pi = 2.22$ MHz. Plotted are contours for $u_z(x, y, z)$ on which $\epsilon_{zz}(x, y, z)$ is color coded at a time of maximum axial extension, where $u_z(x, y, z) = 0$ absent excitation. The phase for propagation from $z = z_R$ to the substrate and back is modified by surface motion u_z at $z = 0$. (b) Coating stack for a high reflectivity mirror with embedded FP cavity for high strain sensitivity.

reflected field is then $\delta\Phi = \delta\theta + \delta\beta$, with $|\delta\beta| \ll |\delta\theta|$ for typical optical coatings. We now present new designs for the coating to achieve $\delta\Phi = \delta\theta + \delta\beta \approx \delta\theta/Q_0$.

The coating structure shown in Fig. 1(b) has an embedded resonant layer that gives rise to a rapid phase variation near the cavity resonance [29]. Explicitly, the coating structure is specified as $n_0(\eta_1\eta_2)^l\eta_1(j \times \eta_{FP}) \times (\eta_1\eta_2)^{p-l}n_s$. Starting from the vacuum side $n_0 = 1$, there are l double layers $(\eta_1\eta_2)^l$ with $\eta_{1,2} = \pi/2$ at the reference wave vector k_0 , followed by an n_1 layer with $\eta_1 = \pi/2$ at k_0 , then the FP n_1 layer with single-pass phase shift $j \times \eta_{FP}$ at k_0 , followed by the terminating $p - l$ double layers, and last the substrate with index n_s . To simplify our discussion, we restrict attention to the case of a “thin” coating with thickness $d \ll a, w_0$ and assume that the axial strain in the coating ϵ_{zz}^c equals that at the substrate’s surface. See Refs. [22,24] for detailed treatments of multilayer coatings. We stress that axial and *transverse* strains are explicitly evaluated for the eigenmode $\xi_0(\mathbf{r})$, including index changes by way of the strain-optic tensor p_{ij} . A discussion of thermal noise from the coating itself is deferred to the conclusion.

Results for two particular coatings are given in Fig. 2 for $w_0 \ll a$. For definiteness, we assume a coating stack made from layers of SiO_2 with index $n_1 = 1.45$ and Ta_2O_5 with $n_2 = 2.03$. Parts (a),(b) are appropriate to $\xi_0(\mathbf{r})$ in Fig. 1(a) with coating structure [$p = 33, l = 8$]. In (a), increased length for the resonant structure leads to greater strain sensitivity, with $|\delta\beta|$ becoming larger relative to $|\delta\theta|$. For $j = 16$ there arise “magic” wave vectors k_{\pm} for which $\delta\Phi(k_{\pm}) = 0$, with the piston phase $\delta\theta$ from surface fluctuations dynamically compensated by the strain-induced coating phase $\delta\beta$. At these “magic wavelengths,” the phase of the reflected optical field becomes insensitive to the thermal motion of the surface of the substrate.

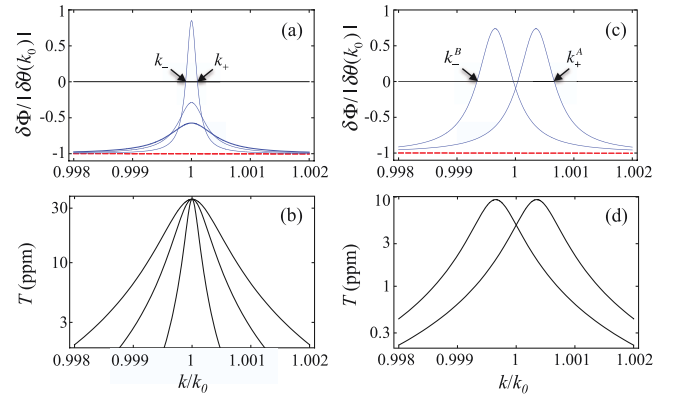


FIG. 2 (color online). Phase shift $\delta\Phi(k)$ and transmission coefficient $T(k)$ for two different coatings illustrated in Fig. 1(b) and specified in the text. (a),(b) The case $\zeta = -1600/\text{m}$ for increasing phase $j\eta_{FP}$ of the internal resonant structure. (a) Total phase $\delta\Phi(k)$ with “magic” wave vectors k_{\pm} and (b) associated transmission coefficient $T(k)$ for $j = 1, 4, 16$ with $\eta_{FP} = \pi$ from widest to narrowest curves. (c),(d) $\delta\Phi(k)$ and $T(k)$ for the case $\zeta = -5000/\text{m}$ for two coatings with slightly different internal resonances $\eta_{FP}^{(A,B)}$ with distinct values k_-^B, k_+^A for nulling noise from mirrors B, A . In all cases, $\delta\Phi(k)/|\delta\theta(k_0)|$ is plotted for $q_0 > 0$, with $\delta\theta(k)$ given by the dashed lines in (a),(c).

Figures 2(c) and 2(d) investigate the possibility that thermal noise of individual mirrors of an interferometer could be measured *in situ*. The coating for each of two mirrors A, B is specified by [$p = 33, l = 7, j = 8$]. The thicknesses of the FP layers in the A, B coatings have been adjusted to give $\eta_{FP}^{(A,B)} = (0.9995, 1.0005)\pi$ at k_0 for the two traces shown. For operation at the lower (upper) value $k_-^B (k_+^A)$ noise from $B(A)$ would be nulled while that from $A(B)$ would be $\sim 80\%$ of the full piston phase, so that the noise arising from mirrors A, B could be individually measured. For operation at $k/k_0 = 1$, thermal noise from A and B would be suppressed. Panel (d) gives the transmission $T(k) = 1 - R(k)$ for the two coatings, where $T(k_-^B, k_+^A)$ is consistent with high-finesse measurements. FP resonances away from $k \approx k_0$ can also be employed to suppress thermal noise. The process control required for these coatings can be addressed with current technology.

Because the surface strain $|\zeta|$ decreases with increasing size of the substrate, compensation of the piston phase $\delta\theta$ with increasing a, w_0 requires greater departures from standard coating designs, material specifications, and fabrication procedures. Moreover, not all eigenmodes of oscillation have the proper parity (i.e., $\zeta < 0$) for compensation by way of the coating designs in Fig. 2.

A second, more challenging example is thermal noise at frequencies ω well below the lowest resonance of the mirror substrate. In this quasistatic regime, we must understand the correlation between thermal displacements at depth z and fluctuations of the surface arising from many modes [11]. The foundation for our analysis is the FDT [7,8] as applied by Levin to this setting [13].

We consider a substrate in the form of an infinite half-space with boundary at $z = 0$ and extending to $z \geq 0$. Equation (9) in Mindlin [30] provides the Green's function required to deduce the admittance for application of the FDT from Eq. (6.8) of Ref. [8]. Following Ref. [15], we find the spectral correlation for beam-averaged axial displacements $\tilde{q}(z)$ at depths z_1, z_2 to be

$$\langle \tilde{q}(z_2)\tilde{q}(z_1) \rangle_\omega = \langle \tilde{q}_0\tilde{q}_0 \rangle_\omega N(z_2, z_1), \quad (1)$$

where $\tilde{q}(z_i) \equiv \tilde{q}(z_i, \omega)$ is the Fourier transform of $q(z_i, t)$. $\langle \tilde{q}_0\tilde{q}_0 \rangle_\omega = 2k_B T(1 - \sigma^2)\phi_s/\pi^{3/2}w_0E\omega$ is the standard result for thermally driven surface displacements, with E, σ the Young's modulus and Poisson ratio, respectively, and ϕ_s the substrate's loss angle. $N(z_2, z_1)$ determines the mechanical admittance and is given by

$$N(z_2, z_1) = \frac{w_0}{8\sqrt{\pi}(1 - \sigma^2)} \int_0^\infty dke^{-k^2w_0^2/4} f(z_2, z_1; k),$$

$$f(z_2, z_1; k) = e^{-k|z_-|}[3 - 4\sigma + k|z_-|] + e^{-kz_+}[5 - 12\sigma + 8\sigma^2 + k(3 - 4\sigma)z_+ + 2k^2z_1z_2], \quad (2)$$

with $z_\pm = z_1 \pm z_2$ and $N(z, z)$ plotted in Fig. 3(a). Here, $N(0, 0) = 1$, $N(z_1, z_2) = N(z_2, z_1)$ [9], and $\langle \tilde{q}(z_1)\tilde{q}(z_1) \rangle_\omega$ in Eq. (1) agrees with previous work [13,15,16].

Spectral correlations between thermally driven axial displacements at depths z_1, z_2 are characterized by [31]

$$C(z_1, z_2) = \frac{\langle \tilde{q}(z_1)\tilde{q}(z_2) \rangle}{\langle \tilde{q}(z_1)\tilde{q}(z_1) \rangle^{1/2} \langle \tilde{q}(z_2)\tilde{q}(z_2) \rangle^{1/2}}, \quad (3)$$

where $C(z, z) = 1$ and $|C(z_1, z_2)| \leq 1$. From Eq. (1) and Fig. 3(a), we see that thermal fluctuations of $\tilde{q}(z)$ correlate over length scales set by w_0 , albeit with decreasing amplitude $\langle \tilde{q}(z)\tilde{q}(z) \rangle \propto N(z, z)$ away from the surface.

Figure 3(b) investigates correlation between displacement $\tilde{q}(z_1)$ at z_1 and axial strain at depth z_2 by way of the function $Q(z_1; z_2, \Delta z_2) = \varepsilon_z^{\text{coh}}(z_1, z_2)/\varepsilon_z^{\text{tot}}(z_2, \Delta z_2)$, with $|Q| \leq 1$. Here, $\varepsilon_z^{\text{coh}}(z_1, z_2) \equiv \langle \tilde{q}(z_1)[\tilde{q}(z_2 + \Delta z_2) - \tilde{q}(z_2)]/\Delta z_2 \rangle / \langle \tilde{q}(z_1)^2 \rangle^{1/2}$ is the strain at z_2 correlated with the displacement $\tilde{q}(z_1)$ at z_1 , while $\varepsilon_z^{\text{tot}}(z_2, \Delta z_2) \equiv \langle [\tilde{q}(z_2 + \Delta z_2) - \tilde{q}(z_2)]^2 \rangle^{1/2} / \Delta z_2$ is the total strain at z_2 .

In Fig. 3(b), the spatial scale for correlation of displacement and strain is again set by w_0 , but now with magnitude reduced by $\sqrt{\Delta z_2/w_0}$. This scaling of Q arises because the rms strain diverges as $1/\sqrt{V}$ for thermal fluctuations in a volume V [32], which motivates our use of finite differences to characterize strain. Near the surface with $\Delta z/w_0 \ll 1$, we find from Eq. (1) that $\varepsilon_z^{\text{tot}}(z \approx 0, \Delta z) \sim [\langle \tilde{q}_0\tilde{q}_0 \rangle / (\Delta z w_0)]^{1/2}$, where the relevant volume $V \sim \pi w_0^2 \Delta z$. By contrast, the coherent strain $\varepsilon_z^{\text{coh}} \equiv \varepsilon_z^{\text{coh}}(0, 0) \sim -\langle \tilde{q}_0\tilde{q}_0 \rangle^{1/2} / w_0$, so that $|\varepsilon_z^{\text{coh}}/\varepsilon_z^{\text{tot}}| \propto \sqrt{\Delta z/w_0} \ll 1$.

From these exact, 3D results for an elastic half-space, we find that thermally driven surface motion \tilde{q}_0 arises from substrate strains over distances $z \gtrsim w_0$. Hence, an optical coating of thickness $\Delta z = d \ll w_0$ employed as a surface-

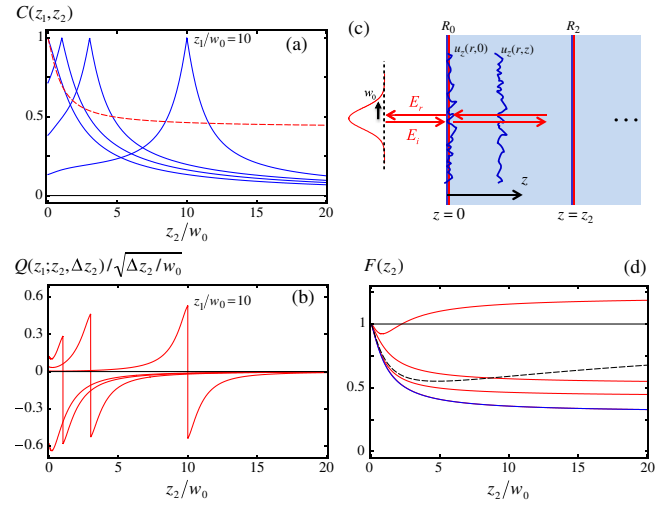


FIG. 3 (color online). (a) Correlation of thermally driven axial displacements $C(z_1, z_2)$ and (b) displacement-strain correlation $Q(z_1; z_2, \Delta z_2)/\sqrt{\Delta z_2/w_0}$ versus z_2/w_0 for $z_1/w_0 = 0, 1, 3, 10$, with $\Delta z_2/w_0 = 10^{-3}$ in (b). The dashed trace in (a) is $N(z_2, z_2)$. (c) Illustration of the mirror geometry discussed in the text. (d) Spectral density of phase fluctuations $F(z_2)$ for the reflected field E_r in (c) for an SiO_2 substrate. From top to bottom, $\alpha = 1.5, 0.3, 1.0, 0.7$ with the blue trace for $\alpha = \alpha_{\text{min}}$ overlaying the curve for $\alpha = 0.7$. The dashed curve is from a simple model that incorporates incoherent contributions from transverse strains to $\delta\beta$. All curves are for $\sigma = 0.2$.

strain sensor as in Fig. 2 will compensate only a small fraction of the phase shift $\delta\theta = -2k\tilde{q}_0$ from the surface motion. Instead, we require a geometry for which $\delta\beta$ has contributions over $z \gtrsim w_0$ sufficient to compensate $\delta\theta$.

Figure 3(c) illustrates a mirror geometry that attempts to achieve such compensation. A thin dielectric coating with reflectivity R_0 is deposited on the substrate's surface, and a second surface is embedded at $z = z_2 \ll nk w_0^2/2$ with reflectivity $R_2 \rightarrow 1$. In the static case, an incident field E_i linearly polarized along x is reflected from this two-mirror geometry to give a field $E_r/E_i = A e^{i\Gamma(\varphi)}$, where φ is the round-trip, internal phase, and $A = 1$ for $R_2 = 1$. Thermally driven fluctuations lead to a phase shift $\delta\Phi = -2k[\tilde{q}_0 + \alpha(k)(\tilde{q}(z_2) - \tilde{q}_0)]$ for E_r , where the piston phase is $\delta\theta = -2k\tilde{q}_0$ and the interferometer phase is $\delta\beta = -2k\alpha(k)(\tilde{q}(z_2) - \tilde{q}_0)$. $\alpha(k)$ expresses the sensitivity of the composite cavity R_0, R_2 to strain driven changes in both length and index around φ_0 , with

$$\alpha(k) = n_s \left(1 - \frac{n_s^2 p_{12}}{2} \right) \left| \frac{d\Gamma(\varphi_0)}{d\varphi} \right|, \quad (4)$$

where p_{12} is an element of the strain-optic tensor p_{ij} and contributions from fluctuating strains transverse to z are neglected and considered below.

We thus find the spectral density of phase fluctuations for the reflected field E_r , namely $\langle (\delta\Phi)^2 \rangle = \langle (\delta\theta)^2 \rangle [(1 - \alpha)^2 + 2\alpha(1 - \alpha)N(0, z_2) + \alpha^2 N(z_2, z_2)]$. Figure 3(d) plots $F(z_2) \equiv \langle (\delta\Phi)^2 \rangle / \langle (\delta\theta)^2 \rangle$ for several values of α . For fixed R_0 with $R_2 = 1$, $\alpha(k)$ varies periodically from

minimum to maximum over the range $\Delta k = \pi/n_s z_2$, with a particular α determined by the choice of k . $F < 1$ represents phase noise reduced below that from thermal fluctuations in the piston phase $\langle(\delta\theta)^2\rangle$. Note that $\alpha = 1$ corresponds to direct compensation of the piston phase $\delta\theta \propto \tilde{q}_0$ for the reflected field, albeit at the price of noise $\tilde{q}(z_2)$ from fluctuations of the reflecting surface at z_2 . More generally, the minimum F_{\min} for given z_2 represents a compromise in noise from \tilde{q}_0 and $\tilde{q}(z_2)$ determined by α_{\min} . $F_{\min} \approx 0.36$ for $z_2 \gg w_0$ in Fig. 3(d).

An important caveat for Fig. 3(d) is that the full curves omit fluctuations arising from transverse strains ϵ_{xx} , ϵ_{yy} , which contribute via p_{ij} to $\delta\beta$ and produce a scaling $F \sim z_2/w_0$ for $z_2/w_0 \gg 1$. A full treatment of these effects is beyond our current analysis. Instead, the dashed curve in Fig. 3(d) is from a simple model based upon the FDT applied to ϵ_{xx} , ϵ_{yy} with loss angle ϕ_s and provides a rough estimate of their incoherent contribution to $\delta\beta$.

The conceptual design in Fig. 3(c) is likely far from optimal. Because the strain field associated with $\psi(r)$ at $z = 0$ spreads transversely for $z > 0$, it is not well matched to our assumed optical profile with fixed $w(z) = w_0$. Geometries with partially reflecting surfaces distributed along z might further reduce F . For finite thickness of the substrate, a treatment as in [15] is required, with now the possibility of reflection from the rear surface [27]. More generally, coherent measurements over a range of k values could enhance sensitivity since $\delta\beta(k)$ can be tailored to be distinct from $\delta\theta(k)$.

Although our treatment has been for substrate ‘‘Brownian’’ noise, our methods should be relevant to the suppression of thermal fluctuations from other sources within the substrate [15,17,18]. Moreover, variations in the design from Fig. 2 could lead to schemes for suppression of thermal noise within the coating [22]. In contrast to the substrate where strains at $z \ll w_0$ have small correlation with \tilde{q}_0 in the quasistatic regime, coating noise produces surface strains that are highly correlated with \tilde{q}_0 .

Important questions remain about our proposals for noise compensation, including significant fabrication challenges, the additional optical absorption within the coating and substrate, and the need for more complete theoretical analyses. We make no claim of a ‘‘magic bullet’’ for eliminating thermal fluctuations. Rather, our goal is to move beyond a surface-centric view and an incoherent summing of noises to consider instead the coherent character of the underlying stochastic displacements and strains and thereby to suggest new strategies for enhanced sensitivity of optical interferometers.

We gratefully acknowledge the critical insights of K. Thorne, as well as valuable discussions with V. Braginsky, Y. Chen, J. Hall, R. Lalezari, F. Khalili, D. Nelson, and S. Vyatchanin. H. J. K.’s work was made possible by JILA. This research is supported by the NSF and NRC.

Note added.—Subsequent to submission and posting of our work, two manuscripts were posted using coherent

effects in optical coatings for reduction of thermal noise [33,34].

*Permanent address: California Institute of Technology MC 12-33, Pasadena, CA 91125, USA.

†Permanent address: Department of Physics, University of Illinois, 1110 West Green Street, Urbana, IL 61801, USA.

- [1] V. B. Braginsky and V. P. Mitrofanov, *Systems with Small Dissipation* (University of Chicago Press, Chicago, 1986).
- [2] K. Numata *et al.*, Phys. Rev. Lett. **91**, 260602 (2003); **93**, 250602 (2004).
- [3] A. D. Ludlow *et al.*, Opt. Lett. **32**, 641 (2007).
- [4] B. C. Barish and R. Weiss, Phys. Today **52**, No. 10, 44 (1999).
- [5] S. Rowan, J. Hough, and D. R. M. Crooks, Phys. Lett. A **347**, 25 (2005).
- [6] F. Marquardt, A. A. Clerk, and S. M. Girvin, arXiv:0803.1164.
- [7] H. B. Callen and R. F. Greene, Phys. Rev. **86**, 702 (1952).
- [8] R. F. Greene and H. B. Callen, Phys. Rev. **88**, 1387 (1952).
- [9] L. D. Landau and E. M. Lifshitz, *Statistical Physics* (Elsevier, New York, 2006), Chap. XII.
- [10] P. R. Saulson, Phys. Rev. D **42**, 2437 (1990).
- [11] A. Gillespie and F. Raab, Phys. Rev. D **52**, 577 (1995).
- [12] N. Nakagawa *et al.*, Rev. Sci. Instrum. **68**, 3553 (1997).
- [13] Yu. Levin, Phys. Rev. D **57**, 659 (1998).
- [14] F. Bondu, P. Hello, and J.-Y. Vinet, Phys. Lett. A **246**, 227 (1998).
- [15] Y. Liu and K. Thorne, Phys. Rev. D **62**, 122002 (2000).
- [16] G. M. Harry *et al.*, Classical Quantum Gravity **19**, 897 (2002).
- [17] V. B. Braginsky, M. L. Gorodetsky, and S. P. Vyatchanin, Phys. Lett. A **264**, 1 (1999).
- [18] V. B. Braginsky and S. P. Vyatchanin, Phys. Lett. A **312**, 244 (2003).
- [19] V. B. Braginsky, M. L. Gorodetsky, and S. P. Vyatchanin, Phys. Lett. A **271**, 303 (2000).
- [20] E. D. Black *et al.*, Phys. Lett. A **328**, 1 (2004).
- [21] E. D. Black, A. Villar, and K. G. Libbrecht, Phys. Rev. Lett. **93**, 241101 (2004).
- [22] G. M. Harry *et al.*, Classical Quantum Gravity **24**, 405 (2007).
- [23] S. D. Penn *et al.*, Phys. Lett. A **352**, 3 (2006).
- [24] M. M. Fejer *et al.*, Phys. Rev. D **70**, 082003 (2004).
- [25] V. B. Braginsky and S. P. Vyatchanin, Phys. Lett. A **324**, 345 (2004).
- [26] S. Gossler *et al.*, Phys. Rev. A **76**, 053810 (2007).
- [27] F. Ya. Khalili, Phys. Lett. A **334**, 67 (2005).
- [28] The parameters for Fig. 1 mimic sapphire, but here for an isotropic medium with Poisson’s ratio $\sigma = 0.29$, Young’s modulus $E = 4 \times 10^{11}$ Pa, and density $\rho = 3980$ kg/m³.
- [29] H. A. Macleod *Thin Film Optical Filters* (Taylor & Francis, Inc., London, 2001), 3rd ed.
- [30] R. Mindlin, Physics **7**, 195 (1936).
- [31] For brevity, henceforth we drop the ω subscript for $\langle \rangle_\omega$.
- [32] M. Parrinello and A. Rahman, J. Chem. Phys. **76**, 2662 (1982).
- [33] M. Evans *et al.*, Phys. Rev. D **78**, 102003 (2008).
- [34] M. L. Gorodetsky, arXiv:0809.0438.